Journal of Harbin Engineering University
ISSN: 1006-7043

Vol 46 No. 1
January 2025

Impact of Nano Magnesium AZ61, AZ91 Alloy on Corrosion, Mechanical, and Microstructural Properties under the Process of Laboratory Ball Milling

P. Mansoor [a] , Dr. S.M Dasharath[b*],

School of Mechanical Engineering, Reva university,

Bangalore, Karnataka 560064, India.

Abstract:

The low density and excellent mechanical qualities of magnesium and its alloys, which are widely used, are examined in this paper's investigation of their microstructural, mechanical, and corrosion properties. Most applications for magnesium and its alloys are in the automotive, biomedical, and aerospace industries. The method of using powder metallurgy to increase the efficacy of magnesium was looked into, where the mixed powder is blended and carried out by uni-axial die compaction followed by sintering. This study examines the impact of cold compaction on magnesium alloys AZ61 and AZ91 utilizing ultra-fine-grained (UFG) powder with a particle size of 60 nm that was produced during an 8-hour mechanical ball milling process at room temperature.The coarse nanocrystalline powder is allowed to compact in a die at 40 MPa pressure for 5 minutes, producing a densely packed platelet. 8 hours of sintering were implemented in a tubular vacuum heater at 425^0C, 450^0C, and 475^0C. Results reveal that the grain boundaries of the magnesium AZ61 and AZ91 alloy during cold compaction and sintering are less porous. It was possible to achieve a mechanical hardness of 543Mpa and compressive strength of 173Mpa, both of which were significantly enhanced by increasing sintering temperatures of 475^0C. At 475^0C temperatures, the lowest corrosion resistance value of 0.27 mm. y^{-1} was achieved.

Keywords: Microstructural, Mechanical, Sintering, Corrosion, Potentiodynamic Polarization, Ultra-Fine-Grained Magnesium.

1 Introduction

Non-renewable resources that are conveniently accessible and have stronger and lighter materials for production are needed today. Magnesium and its alloys play a significant role and have the potential to replace aluminum-based alloys as a structural material due to their higher strength. The density of magnesium is 1.74 g/cm^3 [1-4]. Despite having outstanding mechanical qualities, magnesium and its alloys have numerous disadvantages, including low ductility, strength loss at higher temperatures, and weak corrosion resistance. The use of a severe plastic deformation technique helps get beyond these restrictions [5-10].

By incorporating solid atom components through grain refinement to the nanoscale, which is under investigation, magnesium and its alloy are reinforced. Some researchers have successfully created high-strength magnesium through extreme plastic deformation procedures such as Accumulated Roll Bonding, High-Pressure Torsion, Spark Plasma Sintering, Equal Channel Angular pressing, etc. Warm compacting was used to prepare the Mg-12%Al specimen [2-8]. 489Mpa of compaction pressure was used, and the temperature range was 399^0C to 459^0C. Warmly compacted specimens had a strength that was 20 to 30 Mpa greater than coldly compacted specimens; in warmly compacted specimens, there is a noticeable bonding of the powder particles. Cold and hot compacting methods were used to prepare specimens using Pure Mg [9]. The applied pressure and temperature for the cold and hot compaction methods were 500Mpa/room temperature and 500Mpa/4000C, respectively. Porosity was found to be 5% and 0.5% during cold and hot compaction, respectively. Under Hot compaction, proper diffusion and bonding may be visible.

Magnesium plays a significant role in powder metallurgy, and it has an excellent d density of 1.74 g/cm3. In addition to having a low density, magnesium offers a good stiffness-to-weight ratio and many other beneficial qualities [10-15]. Isotactic pressing, hot pressing, spark plasma sintering, cold pressing, and sintering are some of the most popular powder metallurgy technologies. Severe plastic deformation (SPD) techniques, such as extrusion, high-pressure torsion (HPT), and spark plasma sintering (SPS), can enhance the characteristics of powder metallurgy. By refining the grain, the SPD process enhances the materials' mechanical strength qualities. By reducing grain size to nanocrystalline size, previous research has demonstrated better microstructural and mechanical properties of magnesium alloy. To create solidly formed magnesium composites, intensive plastic deformation procedures such as (ECAP, HPT, and SPS) diffused grains through extended severe plastic deformation [16-20].

2 Literature Review

Modern alloys like AZ91 metal matrix composites (MMC), reinforced with carbon nanotubes (CNT) [21], are used to create lightweight cars and airplanes. The composites employed in this study are prepared by cold pressing, heat treatment, and powder metallurgy (ball milling). CNTs are shown to improve mechanical characteristics. The yield strength and ultimate tensile strength are both enhanced by the inclusion of CNTs. The number of CNTs introduced to the AZ91 affects the coefficient frictions [22]. Due to CNT's inherent ability to lubricate itself, it has been discovered that the wear characteristics diminish as CNT content rises. The minor increase in CNTs does, however, result in some wear factors being reduced, which is covered in this study.

A commercial magnesium alloy known as "AZ61" [23] was subjected to both hot extrusion and thermo mechanical processing (TMP) to examine its microstructures and tensile properties.In this work, the TMP allowed for extensive grain refinement because it had two or three hot rolling processes with significant reductions every pass. The results of the research showed that a two-step processing technique involving an initial extrusion phase followed by thermo mechanical processing with a significant reduction in thickness per pass may be used to obtain fine grain size in the magnesium alloy AZ61 [24]. This two-step procedure aims to produce grains with an average size of 10–20 m.

3 Experimental Procedures

3.1 Materials and Sintering Procedure

As matrix materials, commercially pure magnesium (Mg) powders with a 99.6% purity level were used, with an average particle size of 40 m (400 mesh), and AZ61 powders with a composition of 3wt% Al, 1wt% Zn, 0.5wt% Mn, 0.02wt% Si, and the remaining wt% of Mg.

The first step is the mechanical ball milling of the Mg/AZ61 alloy powders using an SPEX 8000 Shaker for 8 hours in an atmosphere of argon. The SPEX 8000 shaker is a high-energy ball mill that grinds powders weighing between 0.2 and 10 grams. Rotating and moving the vial minimizes particle adherence and prevents the need for lubricants. The final particle size after ball milling is 60 nm, with a ball-to-powder ratio of 10:1 and balls with a diameter of 12.7 mm being employed. To identify the particle phases, the compacted powder specimen will be analyzed using a Siemens D5000 X-Ray diffractometer utilizing the CuK radiation method.

Financially available magnesium (Mg) powders with a purity level of 99.6% and an average particle size of 40 m (400 mesh) as well as AZ91 powders with a composition of 3wt% Al, 1wt% Zn, 0.5wt% Mn, 0.02wt% Si, and the remaining wt% of Mg were used as matrix materials and had an average particle size of 10-44 m.

In the beginning, the Mg AZ91 alloy powders are mechanically ball-milled using an SPEX 8000 Shaker. An argon atmosphere for eight hours. The SPEX 8000 shaker is a high-energy ball mill that grinds powders weighing between 0.2 and 10 grams. Lubricants are avoided and powder adherence is minimized by sliding and rotating movements of the vial.

3.2 Characterization

Archimedes' principle was used to calculate the relative bulk density of sintered specimens, and an electronic balancer with a 0.000g accuracy range

was used to ensure correctness. Optical microscopy reveals the morphology of the texture's grain size. The dispersion of the particles in a sintered composite specimen was examined using a scanning electron microscope (SEM). The specimen samples were ground using 1500 grit emery sheets, then polished with less than 1 m thick diamond paste. Acetic pictorial/glycol solution reveals the sintered specimens' grain boundaries.

3.3 Mechanical Tests.

Vickers hardness is measured mechanically using a HUAYIN HVS-1000A testing device with an indent load of 25g and a holding time of 15s. According to ASTM E9 standards, compressive strength was measured using a computer-controlled UTM (UTM Shimadzu TCE-N300A). The indenter was loaded at a rate of 2 mm per minute until fracture occurred. SEM was supposed to identify the reason why the samples' fractography failed.

4 Results and Discussion:

4.1 Microstructure

According to optical microscopic pictures, sintering at temperatures ranging from 425^{0}C to 475^{0}C followed by cold compacting may be seen. It can be seen from the figures that the grain particles are uniformly dispersed and free of pores and particle boundaries. According to Henry Faisal. the densification of Mg-Al takes place at temperatures between 450^{0}C and 460^{0}C. Additionally, evenly spaced grain boundaries with a compressed pressure force of 20 MPa produced a solid link between the reinforcement of magnesium and aluminum. The Siemens D5000 X-Ray diffractometer with CuK radiation and a scan speed rate of 2 m/s will be used to conduct the X-ray diffraction (XRD) process on the polished specimen surface to evaluate the particle phase structure.

Under the optical microscope and SEM observations. At low sintered temperatures around425^{0}C, grain boundaries, and particle boundaries are more pronounced; when temperatures climb to475^{0}C, barriers start to disintegrate. Additionally, the existence of agglomeration brought on by particle adhesion for temperatures can be seen.

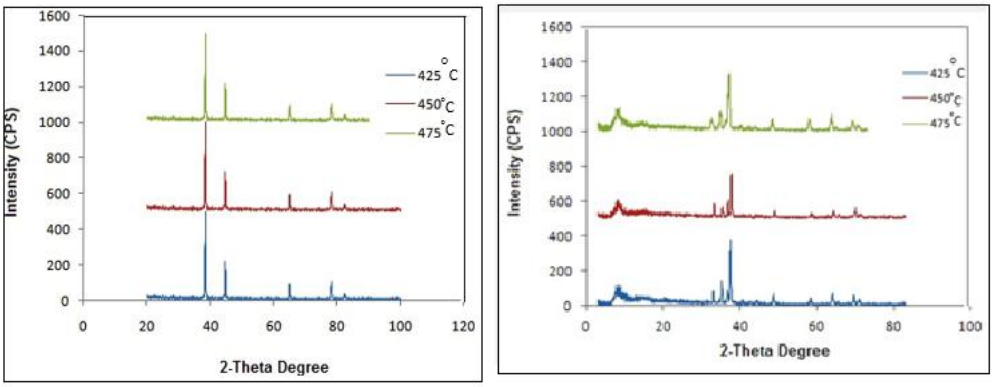

(a) (b)

Figure 1. XRD Patterns for (a) AZ61 and (b) AZ91 alloy samples sintered at a) 425°C b) 450^{0}C c) 475^{0}C

Using an optical microscope, the specimen's structure morphology is observed to examine the grain size and particle structure of the AZ91 and AZ61 alloy.

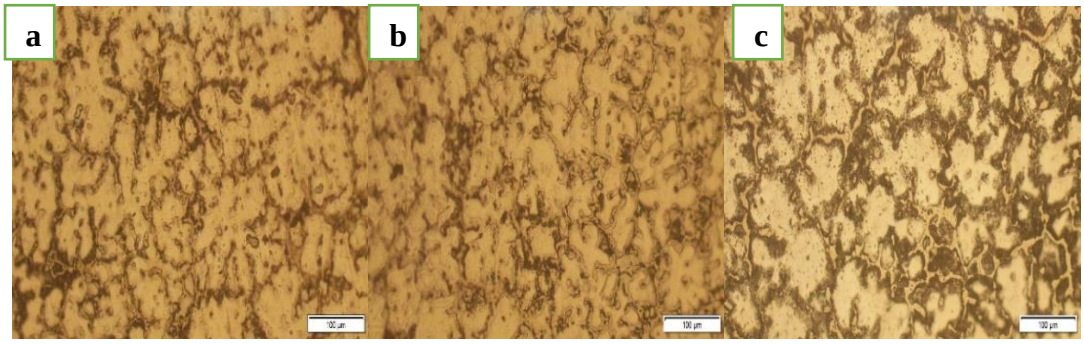

(i) (ii) (iii)

(a)

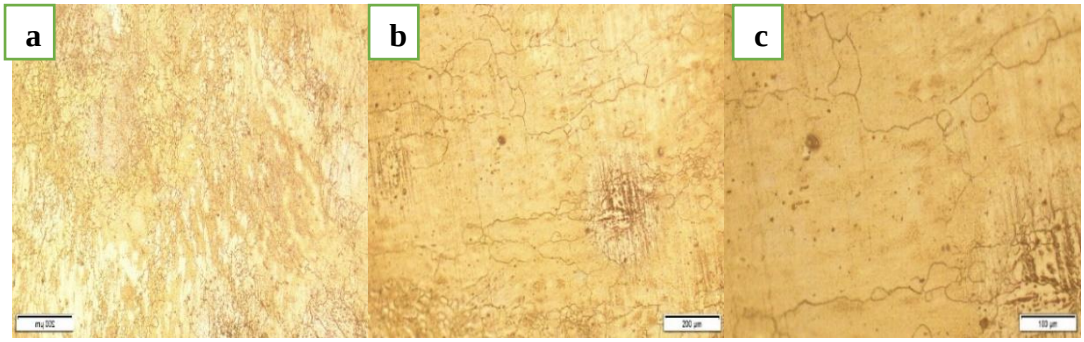

(i) (ii) (iii)

(b)

Figure 2. Optical Microstructures of the (a) AZ91 and (b) AZ61 alloy samples sintered at a)425^{0}C b) 450^{0}C c) 475^{0}C

Under the optical microscope and SEM observations. At low sintered temperatures around 425^{0}C, grain boundaries, and particle boundaries are more pronounced; when temperatures climb to 475^{0}C, barriers start to disintegrate. Additionally, the existence of agglomeration brought on by particle adhesion for temperatures can be seen.

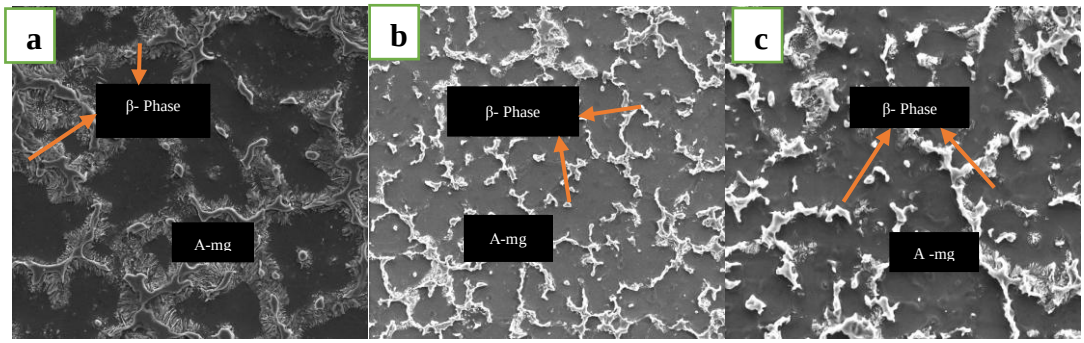

(a)

c

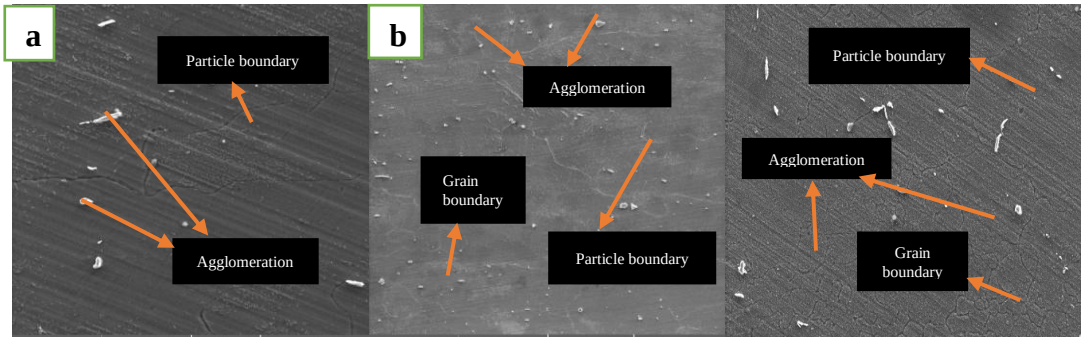

(b)

Figure 3. SEM Morphology of the (a) AZ91 (b) AZ61 alloy samples sintered at a) 425^{0}C b) 450^{0}C c) 475^{0}C

4.2 Relative Density

The Archimedes method was used to determine the relative density for cold compacted sintered AZ61 and AZ91 specimens at various temperatures between 425^{0}C and 475^{0}C. It has been observed that the relative densities for the various temperature ranges are virtually similar. At a sintered temperature of475^{0}C, the highest complete density that was seen was around 98.42%. We can infer from the analysis of the findings that one of the practical processes for producing densified magnesium alloys is cold compaction followed by sintering.

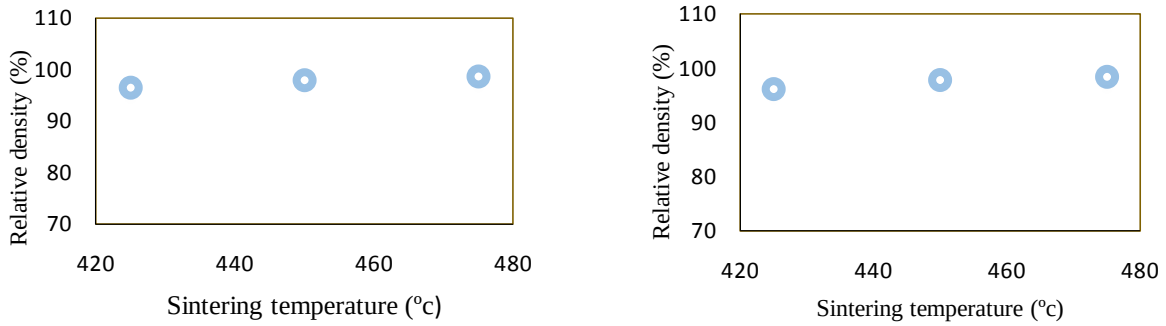

(a) (b)

Figure 4. Relative Density of the (a) AZ91 and (b) AZ61 alloy samples sintered at a) 425^{0}C b) 450^{0}C c) 475^{0}C

Hardness

For magnesium alloys AZ61 and AZ91, the cold compaction process with sintered temperatures ranging from 425^{0}C to 475^{0}C has produced the best mechanical test results. At a temperature of475^{0}C, the highest Vickers hardness measured was around 543Mpa. It should be noted that the ratio of volume to the percentage of relative density and particle size was the reason for the highest hardness. As a result, we can infer that harder materials were produced at higher sintering temperatures due to greater grain bonding and significant particle dislocations at grain borders.

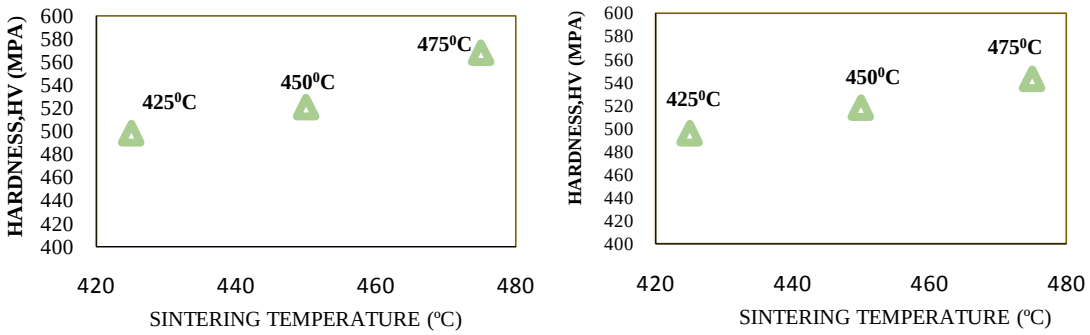

(a) (b)

Figure 5. Hardness of the (a) AZ91 and (b) AZ61 alloy samples sintered at a) 425^{0}C b) 450^{0}C c) 475^{0}C

Compressive Strength

Together with an engineering stress and strain graph, the compressive strength for the specimens of the alloys AZ61 and AZ91 for the temperature range of 425^{0}C to 475^{0}C is measured. It should be noted that at a sintering temperature of 475^{0}C, the greatest peak compressive strength of 173Mpa and strain rate percentage of 23% were obtained. The achievement of full density, which resulted in strong bonding of particles at sintering temperatures of 475^{0}C, was the reason for such the maximum compressive strength. For 425^{0}C and 450^{0}C, the highest yield strength was 109Mpa and 160Mpa, respectively.

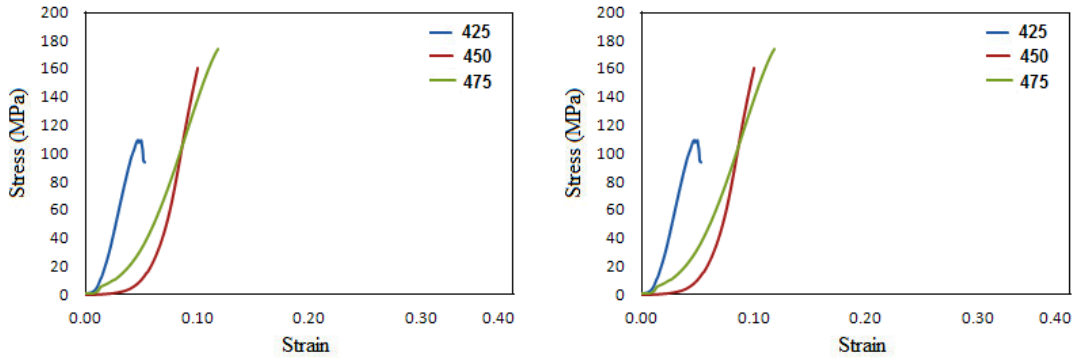

(a) (b)

Figure 6. Compressive strength of the (a) AZ91 (b) AZ61 alloy samples sintered at a) 425^{0}C b) 450^{0}C c) 475^{0}C

Fractography

SEM (Tescan-Vega 3) was used to analyze the fracture morphology of cold compacted and sintered AZ61 and AZ91 alloy specimens at temperatures between 425^{0}C and 475^{0}C. According to observations, failure occurred more frequently when sintering temperatures were lower than 425^{0}C, leading to the formation of fracture-impacting weak borders, porosity, ripping edges, and dimples. The grain boundaries shrank as the sintering temperatures rose, leading to a robust, high densification of grain particles.

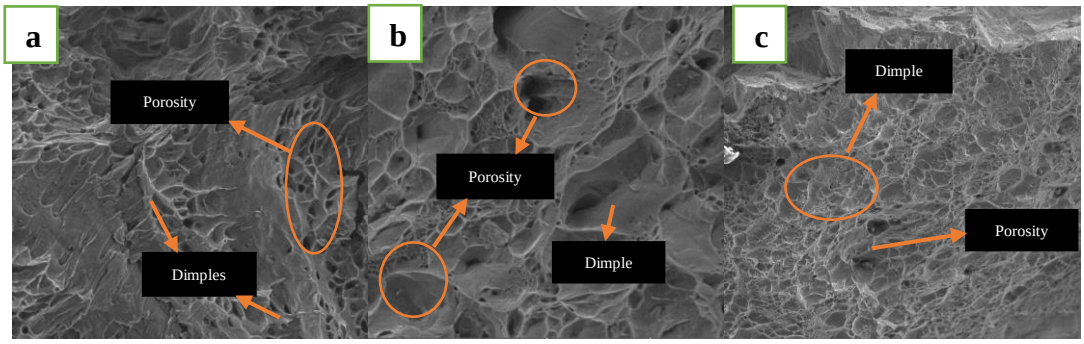

(a)

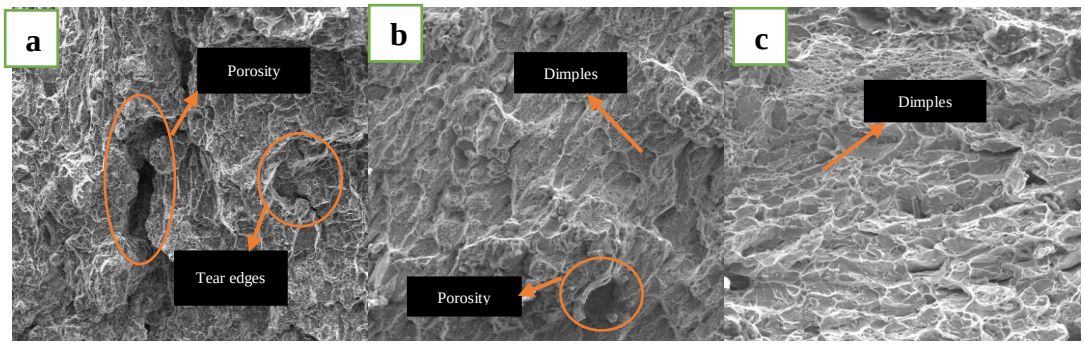

(b)

Figure 7. Facture morphology of the (a) AZ91 and (b) AZ61 alloy samples sintered at a) 425^{0}C b) 450^{0}C c) 475^{0}C

4.3 Potentiodynamic Polarization

Magnesium AZ61 and AZ91 alloy samples were cold compacted and sintered, and potentiodynamic polarisation curves were used to determine the materials' corrosive characteristics in 0.1 M NaCl solution for seven hours of testing. The electrochemical workstation (EC-LAB BIOLOGIC SP-150), has a three-electrode system and includes a saturated calomel electrode (SCE) that serves as the reference electrode, a platinum electrode that serves as the counter electrode, and an electrode that serves as the working electrode for the specimen sample surface that is exposed to a 1 cm^2 area of the electrolyte solution, was used to assess the corrosive properties for sample specimens of the alloy AZ61.The saturated calomel electrode (SCE) vs open circuit potential (OCP) potentiodynamic polarization was carried out at voltages between -200 and +500 mV with a scan rate of 1 mVs-1. The Tafel fit using EC-Lab software will be used to analyze the curves. When compared to various temperatures, it was found that 475^{0}C exhibits the lowest Ecorr of -1.25 mVSCE and color value of 12.76 A.cm-2 as well as the lowest corrosion rate of 0.27 mm.y-1. The table below contains detailed test results for various temperatures. Results of the electrochemical polarisation test 1. Fig 9. The SEM images of the corrosion alloy show less amount of corroded surface at 475^{0}C.

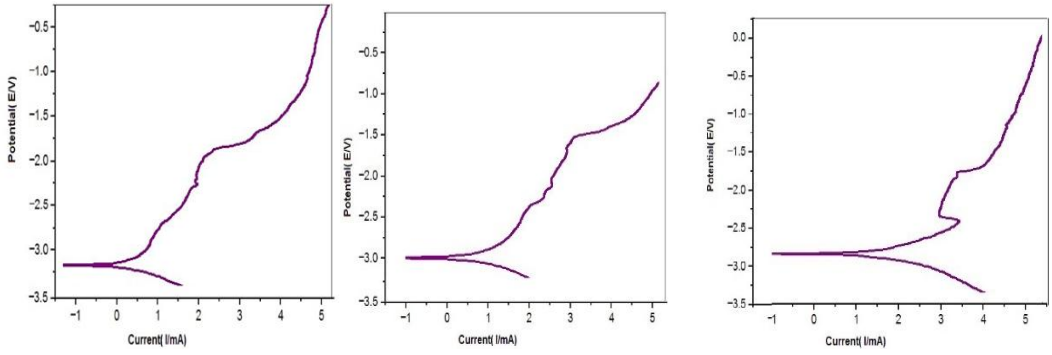

(a)

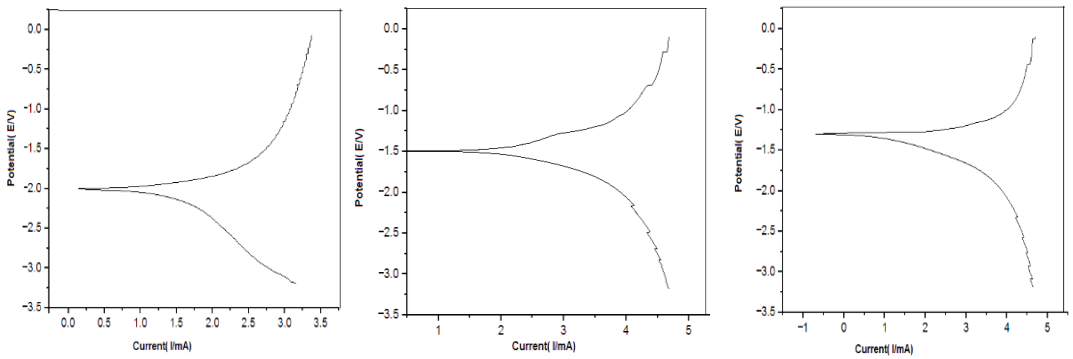

(b)

Figure 8. Potentiodynamic curves of (a) AZ91 and (b) AZ61 alloy samples sintered at a) 425^{0}C b) 450^{0}C c) 475^{0}C

Table 1. Electrochemical Polarization test Results.

Materials	**Sintering Temperatures**	**Ecorr** [mV_{SCE}]	**icorr** [$\mu A.cm^{-2}$]	**rcorr** [$mm.y^{-1}$]
AZ91	425^{0}C	-3.03	97.34	4.45
AZ91	450^{0}C	-3.00	42.62	0.93
AZ91	475^{0}C	-2.56	18.21	0.48
AZ61	425^{0}C	-2.0	85.34	2.76
AZ61	450^{0}C	-1.45	24.35	0.81
AZ61	475^{0}C	-1.25	12.76	0.27

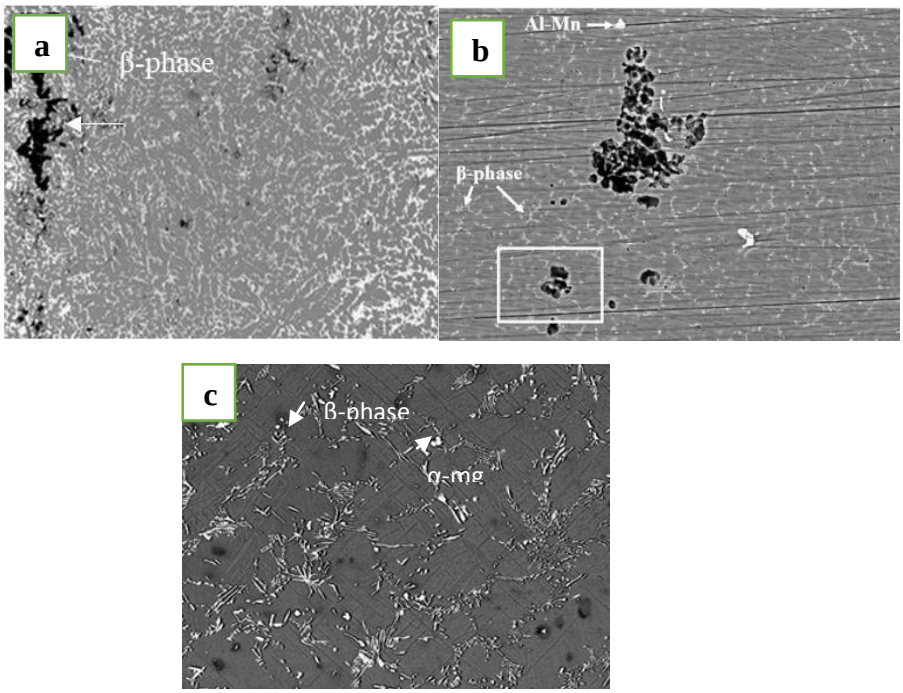

Figure 9. SEM images after Corrosion of (a) AZ91 and (b) AZ61alloy samples sintered at a) 425^{0}C b) 450^{0}C c) 475^{0}C

Conclusion:

The manufacture of densified magnesium AZ61 and AZ91 alloy matrix composites was a successful application of the cold compaction process, followed by sintering. The following is a summary of the observations made during cold compaction and sintering.

1. Under microstructural inspection, homogeneous particle distribution is discovered at higher sintering temperatures of 475^{0}C.
2. Maximum densities are attained at higher sintering temperatures, with the Cold Compacted Sintering Technology reaching a maximum Relative Density of 98.42% at 475^{0}C.
3. At a sintering temperature of 475^{0}C, the mechanical characteristics were significantly enhanced, yielding a hardness of 568 MPa and compressive strength of 182 MPa. Higher properties are attained as a result of the nanostructured UFG powder.
4. By reducing the grain size to a nano size of 60 nm and raising the sintering temperature, the textured surface was improved.
5. Fractography studies showed that the primary causes of failure were inadequate densification and high-phase particles at a lower sintering temperature of 425^{0}C.
6. At a temperature of 475^{0}C, the lowest corrosion rate was recorded at 0.48 and 0.27mm.y^{-1}.

References

[1] Muhammad WNAW, Sajuri Z, Mutoh Y& Miyashita Y,'Microstructure and mechanical properties of magnesium composites prepared by spark plasma sintering technology', *Journal of Alloys and Compounds*, 509(2011) 6021-6029.https://doi.org/10.1016/j.jallcom.2011.02.153

[2] Khan MUF, Patil A, Christudasjustus J, Borkar T &Gupt RK,'Spark plasma sintering of a high-energy ball milled Mg-10 wt% Al alloy', *Journal of Magnesium and Alloys*, 8(2020) 319-328.https://doi.org/10.1016/j.jma.2020.02.006

[3] Pozuelo M, Melnyk C, Kao WH & Yang JM,'Cryomilling and spark plasma sintering of nanocrystalline magnesium-based alloy', *Journal of Materials Research*, 26(2011) 904-911.https://doi.org/10.1557/jmr.2010.94

[4] Karasoglu M, Karaoglu S& Arslan G,'Mechanical properties of Mg-based materials fabricated by mechanical milling and spark plasma sintering', *Proceedings of the Institution of Mechanical Engineers, Part L: Journal of Materials: Design and Applications*, 233(2019) 1972-1984.https://doi.org/10.1177/1464420718805119

[5] Olevsky EA (Ed.). 'Spark-Plasma Sintering and Related Field-Assisted Powder Consolidation Technologies',*Materials*, (2018). https://doi.org/10.3390/books978-3-03842-383-6

[6] Pripanapong P, Umeda J, Imai H, Takahashi M&Kondoh K,'Tensile strength of Ti/Mg alloys dissimilar bonding material fabricated by spark plasma sintering', *International Journal of Engineering Innovations and Research*, 5(2016) 253.http://www.jwri.osaka-u.ac.jp/~dpt6/pdf/project/Topic6-slide4.pdf

[7] Muhammad WNAW, Mutoh Y & Miyashita Y,'Microstructure and mechanical properties of magnesium prepared by spark plasma sintering', In *Advanced Materials Research*, 129(2010) 764-768).https://doi.org/10.4028/www.scientific.net/AMR.129-131.764

[8] Olalekan ON, Abdul Samad M, Hassan SF & Elhady MMI,'Tribological evaluations of spark plasma sintered Mg–Ni composite', *Tribology-Materials, Surfaces & Interfaces*, 16(2022) 110-118.https://doi.org/10.1080/17515831.2021.1898898

[9] Cohen S, Ratzker B, Sokol M, Kalabukhov S & Frage N,'Polycrystalline transparent magnesium aluminate spinel processed by a combination of spark plasma sintering (SPS) and hot isostatic pressing (HIP)', *Journal of the European Ceramic Society*, 38(2018) 5153-5159.https://doi.org/10.1016/j.jeurceramsoc.2018.07.024

[10] Tekumalla S, Si Chun L & Gupta M,'Preprocessing of powder to enhance mechanical and thermal response of bulk magnesium', *Metal Powder Report*, 74(2019) 137-140.https://doi.org/10.1016/j.mprp.2019.03.003

[11] Khodaei M&Toghyani S,'Optimum spacer removal and sintering temperature for porous magnesium scaffold fabrication', *Journal of Tissues and Materials*, 2(2019) 48-57.https://doi.org/10.22034/JTM.2019.188865.1020

[12] Abbas A, Rajagopal V& Huang SJ,'Magnesium metal matrix composites and their applications', *Magnesium alloys structure and properties*, (2021).https://doi.org/10.5772/intechopen.96241

[13] Singh A, Singh J, Sinha MK, Kumar R & Verma V,'Compaction and densification characteristics of iron powder/coal fly ash mixtures processed by powder metallurgy technique', *Journal of Materials Engineering and Performance*, 30(2021) 1207-1220.https://doi.org/10.1007/s11665-020-05429-x

[14] Tun KS, Zhang Y, Parande G, Manakari V & Gupta M'Development of magnesium composites using ball milled high entropy alloy particles', *Indian Journal of Scientific Research*, (2017) 240-245.https://link.gale.com/apps/doc/A531216634/AONE?u=anon~998d3c31&sid=googleScholar&xid=20c064d5

[15] Majzoobi GH, Rahmani K & Kashfi M. 'The effect of pre-compaction on properties of Mg/SiC nanocomposites compacted at high strain rates', *Journal of Stress Analysis*, 4(2020), 19-28.https://doi.org/10.22084/JRSTAN.2019.19874.1105

[16] Kondoh K, Tsuzuki R & Yuasa E. 'Tribological properties of magnesium matrix composite alloys dispersed with Mg 2 Si particles', *Advances in Technology of Materials and Materials Processing Journal*, 7(2005) 33-36.https://doi.org/10.2240/azojomo0110

[17] Clark K, Ehlers J & Wang L, *U.S. Patent No. 6,846,869*. U.S. Patent and Trademark Office,2005.

[18] Dvorský D, Kubásek J, Kristianová E & Vojtěch D, 'Corrosion resistant magnesium-based composite material with MgF2 continuous network prepared by powder metallurgy', *Manufacturing Technology*, 18(2018), 737-741.https://doi.org/10.21062/ujep/169.2018/a/1213-2489/MT/18/5/737

[19] Dvorský D, Kubásek J, Vojtěch D, Voňavková I, Veselý M &Čavojský M,'Structure and mechanical characterization of Mg-Nd-Zn alloys prepared by different processes', in *IOP Conference Series: Materials Science and Engineering,* 179(2017) 012018.https://doi.org/10.1088/1757-899X/179/1/012018

[20] Mondet M, Barraud E, Lemonnier S, Guyon J, Allain N & Grosdidier T. 'Microstructure and mechanical properties of AZ91 magnesium alloy developed by Spark Plasma Sintering', *Acta Materialia*, 119(2016) 55-67.https://doi.org/10.1016/j.actamat.2016.08.006

[21] Upadhyay G, Saxena KK, Sehgal S, Mohammed KA, Prakash C, Dixit S & Buddhi D,'Development of carbon nanotube (CNT)-reinforced Mg alloys: fabrication routes and mechanical properties',*Metals*, 12(2022) 1392.https://doi.org/10.3390/met12081392

[22] Razavi M, Fathi MH &Meratian M. 'Microstructure, mechanical properties and bio-corrosion evaluation of biodegradable AZ91-FA nanocomposites for biomedical applications', *Materials science and engineering: A*, 527(2010) 6938-6944.https://doi.org/10.1016/j.msea.2010.07.063

[23] Yu H, Sun Y, Hu L, Zhou H & Wan Z. 'Microstructural evolution of AZ61-10 at.% Ti composite powders during mechanical milling',*Materials & Design*, 104(2016) 265-275.https://doi.org/10.1016/j.matdes.2016.05.014

[24] El-Morsy A, Ismail A & Waly M,'Microstructural and mechanical properties evolution of magnesium AZ61 alloy processed through a

combination of extrusion and thermomechanical processes', *Materials Science and Engineering: A*, 486(2008) 528-533.https://doi.org/10.1016/j.msea.2007.09.044.

[25] Ali, Murad, M. A. Hussein, and N. Al-Aqeeli. "Magnesium-based composites and alloys for medical applications: A review of mechanical and corrosion properties." Journal of Alloys and Compounds 792 (2019): 1162-1190.

[26] Ogunbiyi, Olugbenga, et al. "Microstructure, Mechanical, Tribological and Synergistic strengthening mechanisms of nickel/graphene nanoplatelets hybrid reinforced AZ91D magnesium-based matrix composites via spark plasma sintering." Journal of Materials Research and Technology (2024).

[27] Fang, Bo, et al. "Effect of nano-sized Mo particles on microstructure and mechanical properties of Mo/AZ31 composites." Materials Science and Engineering: A 893 (2024): 146126.

[28] Shuai, Cijun, et al. "3D honeycomb nanostructure-encapsulated magnesium alloys with superior corrosion resistance and mechanical properties." Composites Part B: Engineering 162 (2019): 611-620.

[29] Ponhan, Kowit. Development of metal matrix nanocomposite based on AZ91 magnesium alloy using conventional stir casting assisted ultrasonic treatment processing. Diss. University of Leicester, 2022.

[30] Fayomi, J., et al. "Magnesium-based composite by nano-nucleation of β-Mg17Al12 using spark plasma sintering route for advanced structural application." Journal of Materials Research and Technology 24 (2023): 1547-1561.

[31] Manroo, Suhail Ahmed, Noor Zaman Khan, and Babar Ahmad. "Development of nano-composites on rare-earth Mg-ZE41 alloy via friction stir processing (FSP): microstructure, mechanical, and tribological properties." JOM 74.5 (2022): 2047-2062.

[32] Vignesh, P., et al. "Microstructure, Mechanical, and Electrochemical Corrosion Performance of Ti/HA (Hydroxyapatite) Particles Reinforced Mg-3Zn Squeeze Casted Composites." International Journal of Metalcasting (2023): 1-13.

[33] Esmaily, M., et al. "Fundamentals and advances in magnesium alloy corrosion." Progress in Materials Science 89 (2017): 92-193.

[34] Ercetin, Ali, and Danil Yurievich Pimenov. "Microstructure, mechanical, and corrosion behavior of Al2O3 reinforced Mg2Zn matrix magnesium composites." Materials 14.17 (2021): 4819.

[35] Liu, Long, et al. "Rare earth element yttrium modified Mg-Al-Zn alloy: Microstructure, degradation properties and hardness." Materials 10.5 (2017): 477.

[36] Balasubramani, N., And U. T. S. Pillai. Studies on Grain Refinement and alloying additions on the Microstructure and Mechanical Properties of Mg-8zn-4ai Alloy. Diss. National Institute for Interdisciplinary Science and Technology, 2009.

[37] Ran, Qianwen, et al. "Effect of TiO 2@ Carbon Nanotubes and Praseodymium on the Microhardness and Corrosion Properties of AZ91 Alloy." Metals and Materials International (2021): 1-11.

[38] Chaudry, Umer Masood, Kotiba Hamad, and Jung-Gu Kim. "On the ductility of magnesium based materials: A mini review." Journal of Alloys and Compounds 792 (2019): 652-664.

[39] Polmear, I. J. "Magnesium alloys and applications." Materials science and technology 10.1 (1994): 1-16.

[40] Lakshmikhanth, R. Sasi, and A. K. Lakshminarayanan. "On the mechanical, microstructural, and corrosion properties of pulsed gas tungsten arc and friction stir welded RZ5 rare earth grade magnesium alloy." Materials Research Express 9.12 (2022): 126507.

[41] He, Xiu-li, et al. "Corrosion fatigue behavior of epoxy-coated Mg–3Al–1Zn alloy in gear oil." Transactions of Nonferrous Metals Society of China 24.11 (2014): 3429-3440.

[42] Bohlen, J., et al. "Rolling of magnesium alloys." Advances in Wrought Magnesium Alloys. Woodhead Publishing, 2012. 346-375.

[43] Rahmani, Ramin, Sérgio Ivan Lopes, and Konda Gokuldoss Prashanth. "Selective laser melting and spark plasma sintering: a perspective on functional biomaterials." Journal of Functional Biomaterials 14.10 (2023): 521.

[44] Reddy, Uttam, et al. "Effect of surface roughness induced by milling operation on the corrosion behavior of magnesium alloys." Journal of Materials Engineering and Performance 30 (2021): 7354-7364.

[45] Huang, Song-Jeng, and Aqeel Abbas. "Effects of tungsten disulfide on microstructure and mechanical properties of AZ91 magnesium alloy manufactured by stir casting." Journal of Alloys and Compounds 817 (2020): 153321.